GEOLOGIC MAPPING OF THE KING CRATER REGION WITH AN EMPHASIS ON MELT POND ANATOMY — EVIDENCE FOR SUBSURFACE DRAINAGE ON THE MOON. J. W. Ashley[1], N. DiCarlo[1], A. C. Enns[1], B. R. Hawke[2], H. Hiesinger[3] , M. S. Robinson[1], H. Sato[1], E. J. Speyerer[1], C. H. van der Bogert[3], R. V. Wagner[1], K. E. Young[1], and the LROC Science Team. [1]Lunar Reconnaissance Orbiter Camera, School of Earth and Space Exploration, Arizona State University, Tempe, AZ 85287-3603 (james.ashley@asu.edu); [2]Hawaii Institute of Geophysics and Planetology, University of Hawaii, Honolulu, HI; [3]Institut für Planetologie, Westfälische Wilhelms-Universität, Münster, Germany.

Introduction: King crater is a 77-km-diameter impact feature and Constellation site of interest, located at 5.0°N and 120.5°E on the lunar farside. The crater has a complex relationship with its surrounding environment. In addition to serving as a model for structural analyses of the lunar highlands [e.g., 1], King crater and its associated large (~ 385 km^2) melt pond (located within adjacent Al-Tusi crater to the north-northwest) provide opportunities for study of high volumes of once-molten, dominantly anorthositic material. The Lunar Reconnaissance Orbiter Camera (LROC) Wide Angle Camera (WAC) and Narrow Angle Camera (NAC) [2] imaged the regional King crater area and melt pond surfaces from a nominal 50 km altitude at pixel scales of 100 meters and up to 0.5 meters for the WAC and NAC, respectively. These images were then used to create new geologic maps for both the regional King crater area and the primary melt pond (e.g., Figure 1). A digital elevation model (DEM) was derived (500 m/p) from the WAC images [3], which allows the estimation of 175 m as a maximum depth for the main melt pond. The new images permit improvement upon previous mapping efforts [e.g., 4], while corroborating many former observations [5-7]. Among the latter are: 1) extensive ejecta patterns in the form of dunes, imbricated deceleration lobes and ballistically emplaced secondary deposits; and 2) evidence for flow within the main melt pond, and melt that ponded locally within the crater wall terraces — showing that post-transient crater fault slumping occurred while melt remained free-flowing.

The high resolution (50 cm/p) NAC images show astonishing detail within the main melt pond that raise questions on the extent and behavior of impact melt in general. In addition to flow features and viscoid forms observed in Apollo 10, 16 and Lunar Orbiter images [1, 5, 7] (e.g., Figure 2a), the melt pond is characterized by positive relief features (2b); craters with anomalous morphologies (which include hummocky floors, irregular outlines, and boulder associations, 2c); and negative relief features (2d). No indications of the tabular features interpreted by [7] as intrusive dikes were obvious in our study.

Significance of negative relief features: The melt pond negative relief features express a range of morphologies that can grade into one another. These include linear canyons and sinuous valleys that could be interpreted as extensional cracks [e.g., 5]. However, natural bridges (Figure 2d), moat-like depressions circumscribing many positive relief features, and other features appear too wide to be extension cracks, and are almost certainly the result of melt withdrawal and collapse, indicating some mechanism for drainage while significant volumes of melt remained mobile. One mechanism is melt penetration into subsurface void spaces by gravity-driven infiltration. Such large-scale porosity might conceivably develop during brecciation and the subsurface readjustment that accompanied the King crater impact event. Melt infiltration presents temperature, viscosity, and volumetric problems, however, that require further investigation (e.g. computer modeling and/or experimental analog testing) to understand thoroughly.

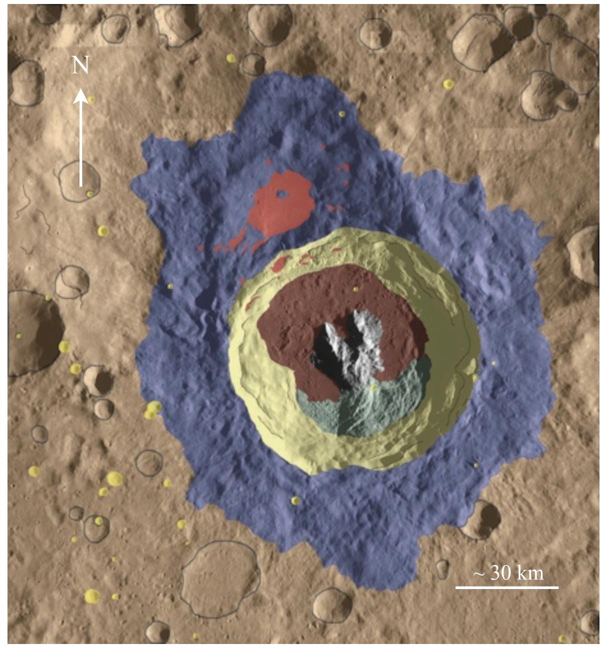

Figure 1. Geologic map of King crater region using a WAC mosaic image base. Major mappable units include proximal ejecta blanket (blue), distal ejecta blanket as decelerated flow material (brown), faulted and slumped crater walls (yellow and green, respectively), central peak (grey), and ponded melt (red toned units). Recent impact craters are represented in dark yellow. Outlines show craters that appear to pre-date the King crater impact event.

Age estimates: Accurate model age determinations for King crater and other young lunar impact features are important for assessing post-heavy bombardment period impact rates, and for correlating global lunar stratigraphy. A count of 9,198 craters confined to a 23 km^2 area on the main melt pond from NAC data yielded an age of ~357 Ma, consistent with the age determination of [8] (counts also from the melt pond) for King crater. However, these ages are incongruent with WAC derived counts on extended and proximal ejecta blanket surfaces, which show King crater to be closer to 1 Ga in age. Speculations on a cause for this age estimate discrepancy include the possibility for differences in target strength, which have been shown to affect crater diameters and thus skew crater counting statistics in other Copernican-aged melt pond situations (e.g., Jackson crater [9], Tycho crater [10]). In addition to material property differences, it is also possible that interference from secondary impacts, the presence of subsurface voids, and the theoretical potential for self-resurfacing, further reduce the applicability of melt surfaces for age determinations using crater counting methods.

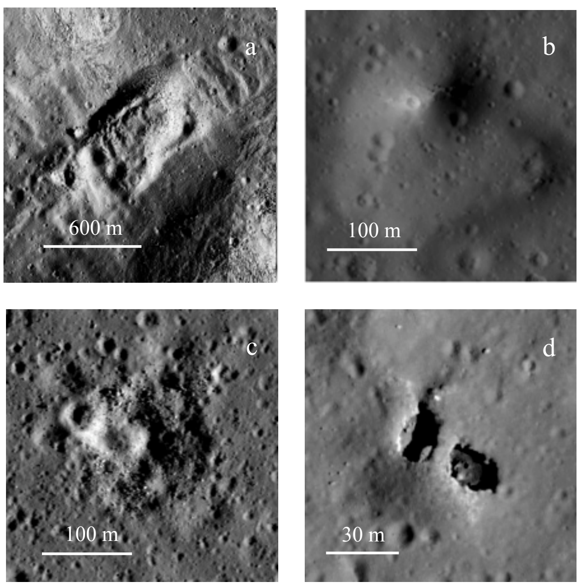

Figure 2. Examples of melt pond features from NAC frames: Viscoid flow feature (a), positive relief feature (b), impact crater with anomalous morphology (c), and negative relief feature (d; representing one of two natural bridges found within the pond). Images: M130863593L/R (a,d); M113168034R (b,c). NASA/GSFC/Arizona State University.

Our WAC count for the proximal ejecta blanket (blue area in Figure 1) excludes the melt pond, and yields an age of ~1.1 ± 0.4 Ga based on the chronology of [11, 12] (Figure 3). The crater size-frequency distribution (CSFD) for King crater is similar to that of Copernicus crater. If King crater were indeed as old as Copernicus crater, then its optical maturity (OMAT) [13] should be the same as Copernicus. However interpreting the OMAT for King crater is complicated due to the fact that rays of Giordono Bruno and Necho craters intersect at King crater [e.g., 7].

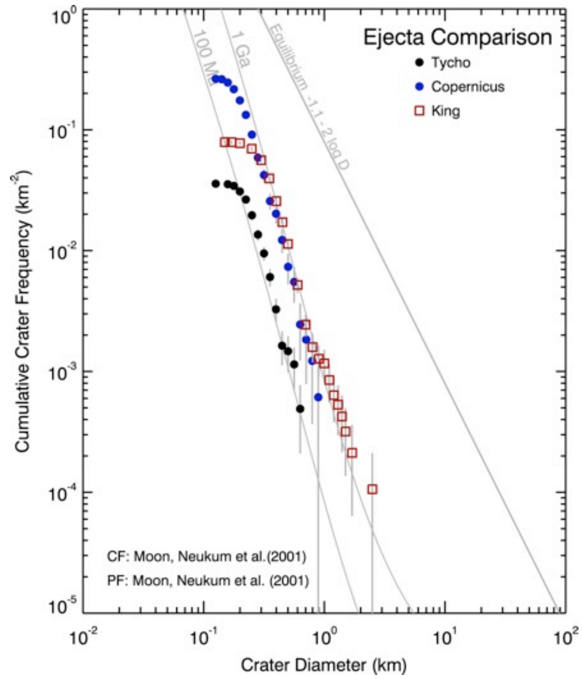

Figure 3. CSFD comparisons for Tycho, Copernicus, and King ejecta blankets using WAC images show King to be of comparable age to Copernicus (~ 1 Ga). Tycho and Copernicus are reference points in the lunar chronology of [12], which are correlated with radiometric and exposure ages from Apollo samples. CSFDs were plotted and fitted using CraterStats [14].

Summary: New high-resolution images and their resulting geologic maps are assisting the interpretation of complex geologic systems on the Moon. NAC images provide the resolution to unravel the complexity of melt pond geomorphology, which shows a surprising variety of surface and subsurface features at King crater, some of which provide evidence for subsurface infiltration of melt while in a molten state. King crater is likely to be ~ 1 Ga in age, but model age determinations remain works in progress.

References: [1] Heather D. J. and Dunkin S. K., (2003) *Icarus* 307-329. [2] Robinson M. S. *et al.*, (2010) *Space Sci. Rev.* 150, 81-124. [3] Scholten *et al.,* (2011) this conference. [4] Wilhelms D. E. and El-baz F. (1977) *USGS,* Map I-948. [5] Howard K. A. (1972) *NASA Apollo 16 PSR,* Part N, 29-70–29-77. [6] Oberbeck V. R. *et al.,* (1972) *NASA Apollo 16 PSR,* Part K, 29-51–29-56. [7] El-baz F. (1972) *NASA Apollo 16 PSR,* Part M, 29-62–29-70. [8] Young R. A. (1977) *LPSC VIII.* [9] van der Bogert C. H. *et al.,* (2010) *LPSC XLI*, abs. #2165. [10] Hiesinger H. *et al.,* (2010) *LPSC XLI,* abs. #2287. [11] Neukum G. and Ivanov B (1994) Hazards due to Comets and Asteroids, 359-416. [12] Neukum G. *et al.,* (2001) *Space Sci. Rev.,* 96, 55-86. [13] Lucey P. G. *et al.,* (2000) *JGR* 105, E8, 20,377–20,386. [14] Neukum G. (2007) *LPSC XXXVIII.*